



École Supérieure de Physique et de Chimie Industrielles de la Ville de Paris

3RD YEAR RESEARCH PROJECT

Quantifying dopamine adhesion via contact angle measurements

Holten-Andersen Lab, Department of Material Science and Engineering, MIT

Student : Thomas Bonazzi

Supervised by : Niels Holten-Andersen
Thibaut Divoux
Martin Lenz

Date : May 7th - July 31st 2018

Acknowledgements

I would like to thank both Thibaut Divoux and Niels Holten-Andersen for their continuous support, patience and availability throughout this internship, as well as Martin Lenz for its eventually much appreciated rigor. They all have been of great help in making this project happen from its conception to this report. I would also like to thank the HML for letting me use their equipment as well as their meeting room for the summer interns' group meetings.

I am also extremely grateful to the joint CNRS/MIT lab $\langle \text{MSE} \rangle^2$ and its director Roland Pellenq, as well as the Fond ESPCI Paris for their financial support, which allowed me to come work at the MIT in the first place. Finally, I am thankful to Annie Colin who will have taken the time to read this report for the ESPCI.

Contents

1	Introduction	3
1.1	Adhesion of the marine mussel to solid substrates	3
1.2	Dopamine	3
1.3	Contact angle measurement to monitor dopamine adhesion	4
2	Materials and methods	5
2.1	Dopamine solution preparation	5
2.2	Contact angle measurement	6
2.2.1	Advancing and receding contact angle	6
2.2.2	Goniometer measurements	7
2.3	Substrates preparation	8
3	Results	9
3.1	Influence of the dopa concentration on different substrates	9
3.2	Multiple hysteresis cycles	10
3.3	Time dependence of the angle	12
4	Discussion	14
4.1	Kinetics of adsorption	14
4.2	Back to adhesion energy	15
5	Conclusion	16

1 Introduction

1.1 Adhesion of the marine mussel to solid substrates

Adhesion of any sort is a major technological field and challenge, and nature has developed many solutions depending on the situation, from the gecko to the barnacle. But adhesion to wet, salt-encrusted, corroded and slimy surfaces remains a major impasse for technology. The marine mussel [Fig. 1(a),(b)], an example of what is achievable in a marine environment, has served as a model over the last four decades for a better understanding of the requirements for such adhesion.

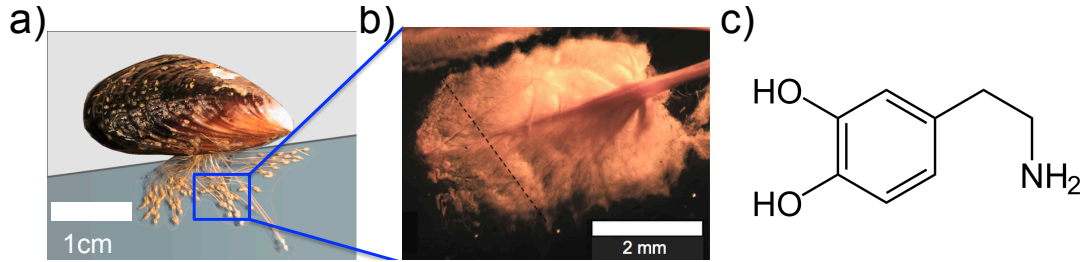


Figure 1: (a) A *Mytilus* mussel byssus contains hundreds of threads proximally fused to muscle at the base of the foot attached to the substrate. (b) Zoomed view of one contact between a thread and the substrate. (c) Skeletal structural formula of the Dopamine. On the left, the catecholic part is responsible for most of the adhesive properties and on the right, the amine group creates cohesive properties.

The actual process of mussel adhesion through its foot and byssus is actually very complicated and involves numerous proteins, pH changes and pressure modifications [1]. Nevertheless, one of the most abundant proteins in the foot, the 3,4-dihydroxyphenyl-L-alanine [Dopa, Fig. 1(c)] is believed to play a crucial role in this adhesion process. This catecholic amino acid Dopa is also found in the cement of sandcastle worms and tunicates, among others [2].

1.2 Dopamine

Dopamine is an organic compound that has a catechol (benzene with two hydroxyl side groups at carbons 1 and 2) and a side-chain amine [Fig. 1(c)]. This relatively simple structure allows nevertheless for many types of reactions with a surface but also with itself, creating both adhesive and cohesive bonds ([3], [4]). The adhesive bonds, interfacial interactions with the substrate implicated include bidentate H-bonding [3], hydrophobic interactions through the aromatic cycle [5] and even coordination for $\text{pH} \geq 5$ [Fig. 2(a)]. Using AFM, Lee *et al.* (2006) [6] measured the strength of a single molecule bonding to metallic substrate in marine-like conditions [Fig. 2(b)] and found a force of 900 pN over 21 nm, which corresponds to an energy of about 113 kJ.mol^{-1} (to be compared for instance with 21 kJ.mol^{-1} for a O-H - - O hydrogen bond, or 348 kJ.mol^{-1} for a covalent C-C bond). This result though, in the case of packed dopamine on a surface, would lead to an adhesion energy of 10 J.m^{-2} at best. This is quite far off from another measure : a simple peeling test of a mussel foot provided with an energy of 200 J.mol^{-1} [1]. Though the mussel has a richer process of adhesion, it still sheds doubt about the actual efficiency of the dopamine regarding adhesion or on our ability to quantify it.

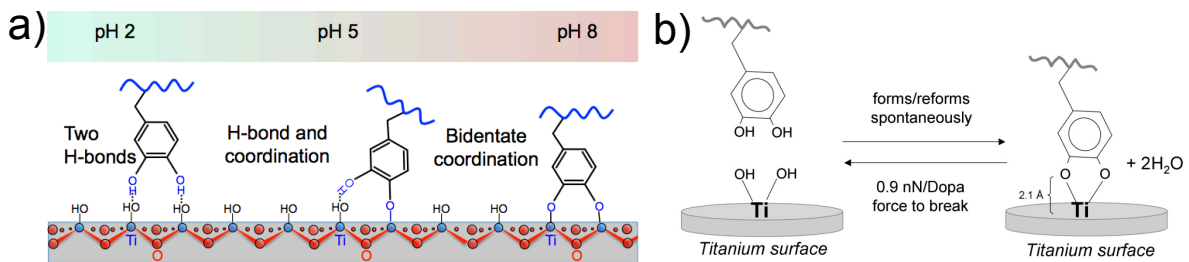


Figure 2: (a) Dopamine adhesion on an oxide layer or metallic surface consists essentially in H-bonds or coordination bonds and depends on the pH. (b) AFM single dopamine molecule pull from a titanium surface. Sketches from Lee *et al.* (2006) [6].

1.3 Contact angle measurement to monitor dopamine adhesion

A drop of liquid on a plane solid surface experiences adhesive forces acting between the liquid and the solid surface that favor spreading, whereas the cohesive forces within the liquid counteract the spreading. When a droplet of liquid is placed on a solid substrate, the shape of the droplet results from an equilibrium between three surface tensions : liquid-vapor γ_{LV} , liquid-solid γ_{LS} and solid-vapor γ_{SV} (Fig. 3). On a flat and smooth surface, the balance of those forces along the contact line around the droplet follows the Young-Dupré law :

$$\gamma_{SV} - \gamma_{LS} = \gamma_{LV} \cdot \cos(\theta_Y) \quad (1)$$

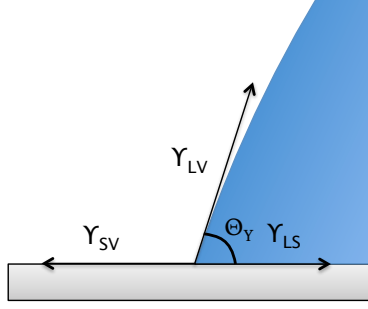


Figure 3: A liquid Droplet at equilibrium on a substrate. the Young angle is unique and is defined by the balance of the three energies : it is the Young-Dupré law.

The surface energy γ_{LS} between the liquid and the substrate is a function of the nature of the interface. This contact angle measure is commonly used to characterize surfaces for instance to evaluate a surface treatment (using reference liquids where the γ_{LV} is well known), but less so to evaluate the adsorption of a molecule onto a substrate. In this context, the value of the contact angle of a dopamine solution might be revealing of the surface state. To be convinced that it is reasonable to expect a change in the contact angles when coating a surface with dopamine, we made some back envelope calculations to estimate the energies at stake.

First let us consider an aqueous dopamine solution with metallic ions in it. An equilibrium between the ions (I), the ligand (L), and the complex ligand-ion (LI) takes place



with the dissociation constant $K_d^{-1} = C_I \cdot C_L / C_{LI}$, where the C_i denote the concentrations in ion, ligand and ligand-ion complex. Let also a be the characteristic size of the Dopa molecule and N_i the amount of each species. Now in an ideal solution we can write the free energy F as follows

$$F = N_L kT \ln(N_L \cdot a^3 / V) + N_I kT \ln(N_I \cdot a^3 / V) + N_{LI} kT \ln(N_{LI} \cdot a^3 / V) - \Delta E \cdot N_{LI} \quad (3)$$

From which we can derive the chemical potentials μ_i
$$\begin{cases} \mu_I = \frac{\partial F}{\partial N_I} = kT \cdot [\ln(C_I a^3)] \\ \mu_L = \frac{\partial F}{\partial N_L} = kT \cdot [\ln(C_L a^3)] \\ \mu_{LI} = \frac{\partial F}{\partial N_{LI}} = kT \cdot [\ln(C_{LI} a^3)] - \Delta E \end{cases} \quad (4)$$

Finally, by equating at equilibrium μ_{LI} and $\mu_I + \mu_L$, we obtain

$$\Delta E = k_B T [-1 - \ln(K_d \cdot a^3)] \quad (5)$$

Using an average value for metallic ions with catechols [7], $K_d < 2.10^{-5} \text{ mol.L}^{-1}$ and estimating $a = 30 \text{ nm}$, that yields eventually at least $\Delta E \simeq -14k_B T$.

Now let us consider the surface A_{tot} , viewed as a squared lattice, of period A_{tot}/a^2 . Let Φ be the fraction of occupied sites by the dopamine molecule. In the grand canonical ensemble, considering the droplet as a reservoir (we will discuss this hypothesis later on), we write

$$F = \underbrace{\frac{A}{a^2} \cdot kT \cdot [\Phi \ln(\Phi) + (1 - \Phi) \ln(1 - \Phi)]}_{entropy} - \underbrace{\frac{\Delta E \cdot \Phi \cdot A}{a^2}}_{adsorption} - \underbrace{\frac{\mu_L \Phi \cdot A}{a^2}}_{reservoir} \quad (6)$$

Given the form of the free energy plotted in Fig. 4, we consider that the minimum is reached for $\Phi = 1$,

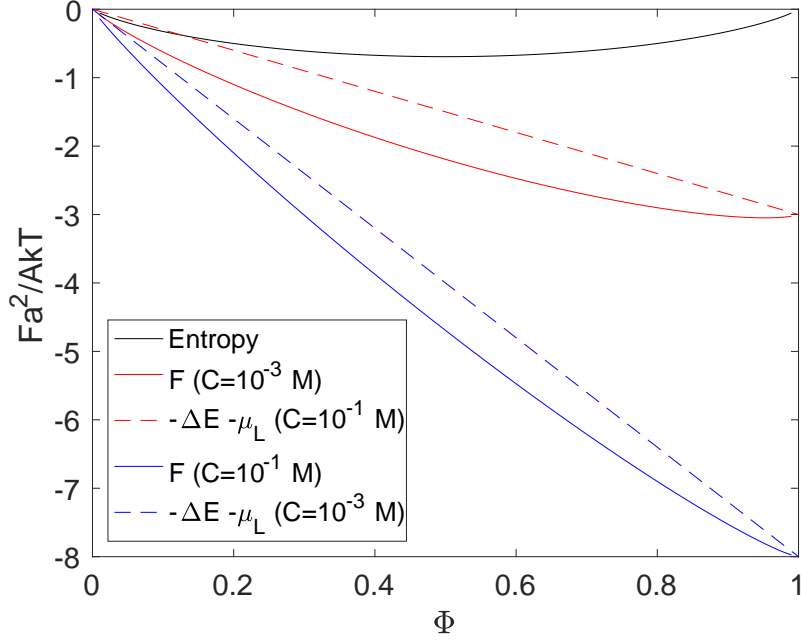


Figure 4: Plot of the free energy per site normalized by kT (dashed lines) in our calculation, as the sum of the entropy term, the adsorption term and the reservoir depletion, versus the fraction of occupied sites, for two concentrations in ligand. It appears that the entropy term is largely dominated by the other terms.

allowing us finally to write

$$\frac{F}{A} = -\frac{1}{a^2} [\Delta E + k_B T \ln(1 + C_L a^3)] \quad (7)$$

Numerically it corresponds to a variation in energy of roughly 1 J.m^{-2} or 1 N.m^{-1} . The surface energy of glass is approximately $0,3 \text{ J.m}^{-2}$, and for iron it is around 2 J.m^{-2} ([8], [9]) This gives reasons to hope for an effect on the contact angles of dopamine solution. To consider the droplet (concentration C) as a reservoir, which means that we have enough molecules to coat the surface without depleting the bulk, of size h , we need the number of molecules to be very large, i.e.

$$Ca^2 h \gg 1 \iff C \gg C_{crit} = \frac{1}{h.a^2} \quad (8)$$

For a generic contact angle experiment, the droplet's height is about 1 mm , so the critical concentration is $C_{crit} = 2.10^{-5} \text{ mol.L}^{-1}$. Under this condition, the droplet can act as a reservoir and we can expect to see some change in the contact angle of our dopamine solution on the substrate.

2 Materials and methods

2.1 Dopamine solution preparation

We used Dopamine aqueous solution ranging from $10^{-1} \text{ mol.L}^{-1}$ to $10^{-8} \text{ mol.L}^{-1}$. The $10^{-1} \text{ mol.L}^{-1}$ Dopamine solution were prepared using $189,6 \text{ mg}$ of Dopamine hydrochloride salt ($M=189,64 \text{ g/mol}$), diluted in 10 mL of deionized water. From there on, less concentrated dopamine solutions were successively prepared by diluting 1 mL of the $10^{-n} \text{ mol.L}^{-1}$ in 9 mL of deionized water to obtain 10 mL of the $10^{-(n+1)} \text{ mol.L}^{-1}$ Concentrations were determined using a DeNovix DS-11 UV-Vis spectrometer. The dopamine UV-vis absorption spectrum is characterized by a high and thin peak at 280 nm [10] (clearly visible in Fig. 5, with an extinction coefficient $\epsilon = 2,7.10^3 \text{ L.mol}^{-1}.\text{cm}^{-1}$ [11]). Only the five most concentrated solutions have been investigated because the sensitivity of the spectrometer only allowed so much. Since the concentration tested were at the correct concentration, we consider the lower one correct also. Since dopamine is supposed to adhere to many substrates [12], the same needle tip was used for the contact angle experiment and the UV-vis spectrometry tests to avoid a bias between the measurement of the spectrum and the others experiments. The most concentrated sample (Fig. 5, inset) seems not concentrated enough though it is the one I actually weighted. This might be the result of the coating of

the needle used for the measure. There is no reason otherwise that this point would be off and then the others prepared with it would be correct. As we will see later, the coating rate increases with the concentration, maybe explaining why this effect is only visible for high concentration. Besides the solution is transparent, so it should not be a saturation of the spectrometer either.

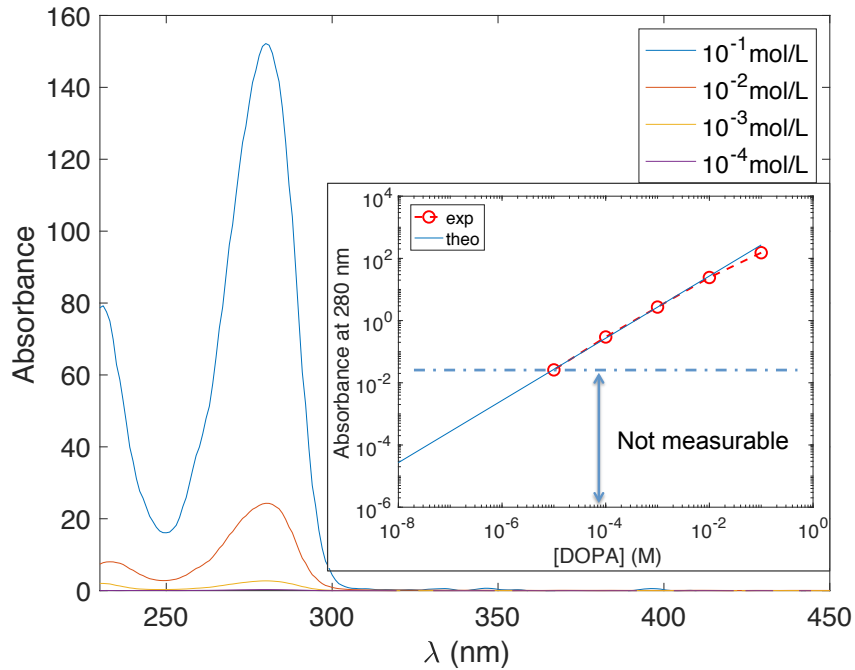


Figure 5: Absorption spectrum of the dopamine solutions for concentrations ranging between $10^{-1} \text{ mol.L}^{-1}$ and $10^{-4} \text{ mol.L}^{-1}$. The peak of absorption at 280 nm is characteristic of the dopamine (and the catechols in general [10]). In the inset, the value of the absorbance at 280 nm and the theoretical expectation for each concentration allows to be confident in our dilution.

2.2 Contact angle measurement

2.2.1 Advancing and receding contact angle

As we have seen before, there exists a thermodynamical equilibrium angle θ_Y , resulting from a balance between the different phases and surface energies. This unique contact angle θ_Y is contradicting our daily experience though : we often see a spectrum of angles. Different drops of the same water on a regular surface can display contact angles varying over more than 10 degrees, especially if moving [13]. (Fig. 6)



Figure 6: Photo of a blade of grass with dewdrops on it, displaying various contact angles.

A real surface is actually very often covered with defects (structural and chemical) that complicate this energy balance locally and "pins" the contact line, making the practical observation of the thermody-

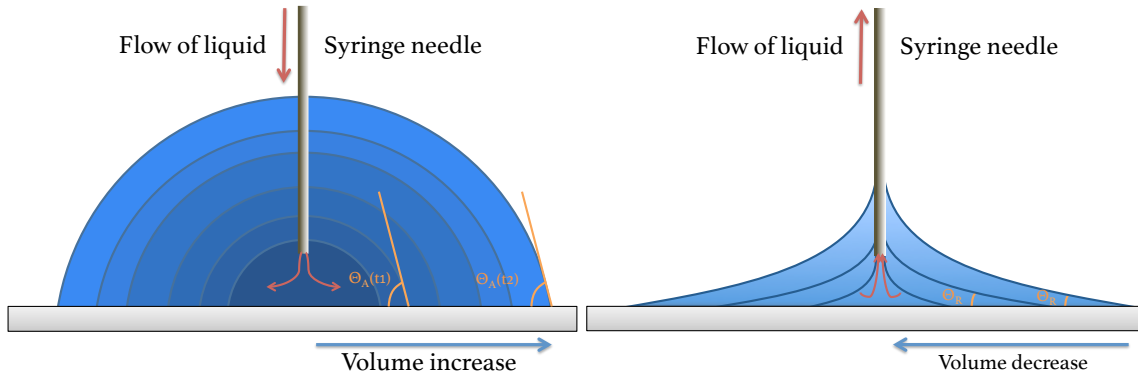


Figure 7: Illustration of the advancing and receding angles while adding or withdrawing liquid. Because it averages the inhomogeneities out, both angles are constant during the experiment.

namical quantity θ_Y tricky. But from this pinning effect arises an hysteresis between the advancing angle θ_A (when we add a little volume to the droplet or at the front when the drop moves) and the receding angle θ_R (when we retrieve a little liquid from the droplet or at the back when the drop moves) as it is shown in Fig. 7. Those two quantities are indeed much more reliable when investigating a surface because they average the local inhomogeneities of the surface. Besides, by continuously adding or withdrawing liquid, we compensate the evaporation of our droplet. At the very beginning of the advancing angle experiment (when the droplet is of same characteristic size as the tip of the needle), the contact angle will vary with the volume of the droplet or the drop size, as the contact with the needle affects the drop's shape.

2.2.2 Goniometer measurements

The advancing and receding angles were measured using a Ramé-Hart Goniometer [Fig. 8(a)]. This instrument consists of a horizontal surface, illuminated by a lamp on one side, and a high resolution camera on the opposite side. A syringe on top of the setup, connected to a precise pump, allows for a controlled deposition of liquid. Advancing and receding angles were generated by respectively adding and withdrawing liquid with the syringe as slowly as the pump allows ($0,25 \mu\text{L}\cdot\text{s}^{-1}$) to avoid any dynamical effects on the shape on the droplet.

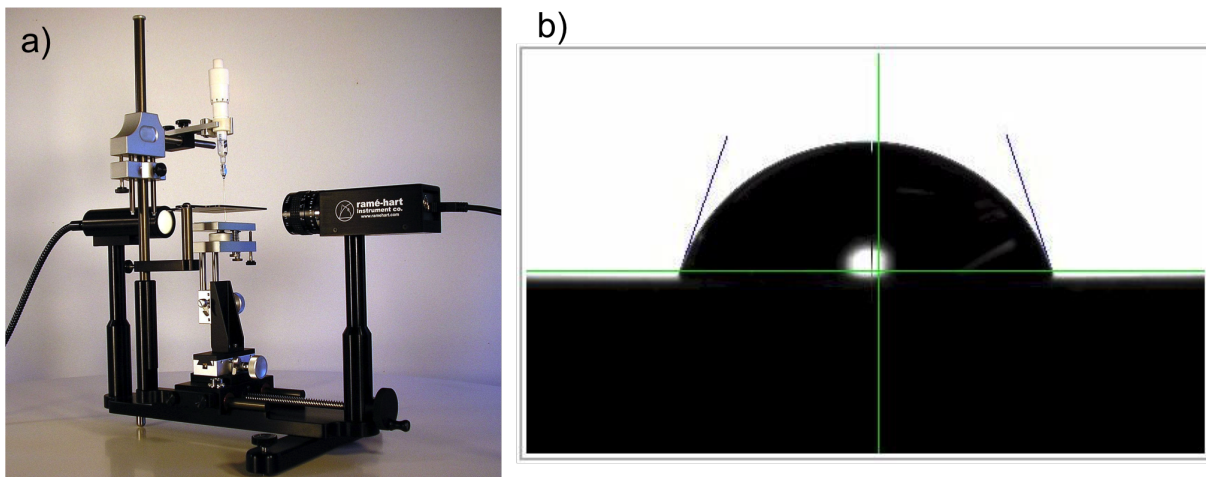


Figure 8: a) Photo of a Ramé-Hart Goniometer. On the right, the camera is able to film the surface positioned under the syringe. The lamp on the left provides a backlighting for a satisfying contrast. Focus can be achieved by sliding the camera along the rail using a precision screw. b) Screenshot of the software DROPimage with the tangents being measured above the baseline (horizontal, green).

A software (DROPimage®) is used to capture and analyze the contact angle. The default method uses a circular curve fit to an adjustable number of the profile points closest to the baseline and calculates the tangent to that circle analytically [Fig. 8(b)]. The software unfortunately was sometime unable to

capture the angle. We tried changing the lighting, the focus, the size of the droplet, but the software really behaved erratically. Manual measurements using ImageJ were then required. Each angle value was averaged over three measurements for precision evaluation. Though more time consuming, this method seems more reliable, especially for low angles ($<10^\circ$), which were often underestimated by the software as Fig. 9(a) shows. The difference between the two ways of measuring are plotted in Fig. 9(b). The average difference of $0,23^\circ$ for angles above 40° is well within any error bars for such measurements so there is no problem with using the software. But for the low angles this difference between the methods is of $3,51^\circ$ on average and with a large standard deviation ($2,4^\circ$), requiring a manual double check before concluding with the software. Knowing that, and with the notable exception of the experiments with multiple cycles of hysteresis described in part 3.2, all measures were done using ImageJ.

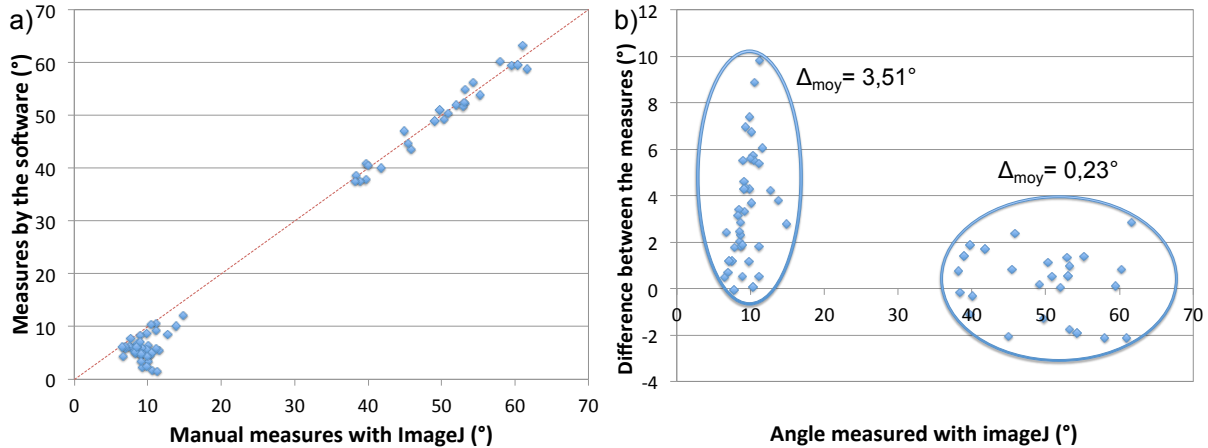


Figure 9: a) Measurements obtained with DROPimage versus measurements done manually with imageJ, during multiples cycles with a solution of dopamine (10^{-1}mol.L^{-1}) on polished steel. The red dashed line is the first bissectrice, along which each point should align if each measurement was perfect. The discrepancy between the two methods, significant for low angles ($<10^\circ$), is best displayed in (b). b) Difference between contact angles measured by the software and manually. It appears that angles around 10° , typical value for the receding angles, are poorly captured by the software.

2.3 Substrates preparation

We have measured contact angle of dopamine solution on various substrates: glass, stainless steel and Polytetrafluoroethylene (PTFE, Teflon®). For the glass, we used microscope slides (ThermoFisher®) without any treatment. Teflon and steel were either used raw or polished to control the roughness of the samples. To do so, we performed manual polishing using abrasive discs of silicon carbide of decreasing roughness, mounted on a rotor (300 tr/min): $35\ \mu\text{m}$, 22, 14, 10 and $5\ \mu\text{m}$ (Buehler®). We finished the polishing by gently brushing the specimen for a minute on a $1\ \mu\text{m}$ abrasive disc mounted on a flat glass surface. The final surface, much more reflective, is shown in Fig. 10. Before any experiments, substrates were sonicated 10 min in acetone. Between each measures, isopropanol and precision wipes served to removed ambient dust that fell on our substrate during the previous experiment.



Figure 10: Comparison between unpolished (left) and polished (right) steel

3 Results

3.1 Influence of the dopa concentration on different substrates

We measured advancing and receding angle of a dopamine solution on glass (microscope slides), for a large range of concentrations, from 10^{-8}mol.L^{-1} to 10^{-1}mol.L^{-1} and we used pure water as a reference. Because the chemistry of the dopamine adhesion to a substrate is known to be pH-dependent [1], two sets of solutions were used : one with dopamine and water ($\text{pH}\simeq 7$) and one with NaOH (1 mol.l^{-1}) added until $\text{pH}=12$ was reached. Only a few μL per mL were necessary so the dilution was negligible. In Fig. 11, 12 and 13, the advancing and receding angles are represented by boxes : the advancing angle is the top of the box, the receding the bottom. Error bars, when available, are displayed on top of it. On the far left part of each graph, an orange zone represents the reference, pure water for $\text{pH}=7$ or water and NaOH for $\text{pH}=12$.

For the glass at $\text{pH}=7$ there is a clear increase of both the advancing and receding angle for increasing DOPA concentration above $10^{-6}\text{ mol.L}^{-1}$, reaching respectively 58° and 21° , where the reference displayed advancing and receding angles of 29° and 8° respectively [Fig 11(a)]. This means that once coated with dopamine, the glass shows a less hydrophilic behavior than uncoated. On the other hand at $\text{pH}=12$ [Fig 11(b)], there seems to be little to no effects of dopamine on contact angles: every measure is seemingly within error bars the same as the reference.

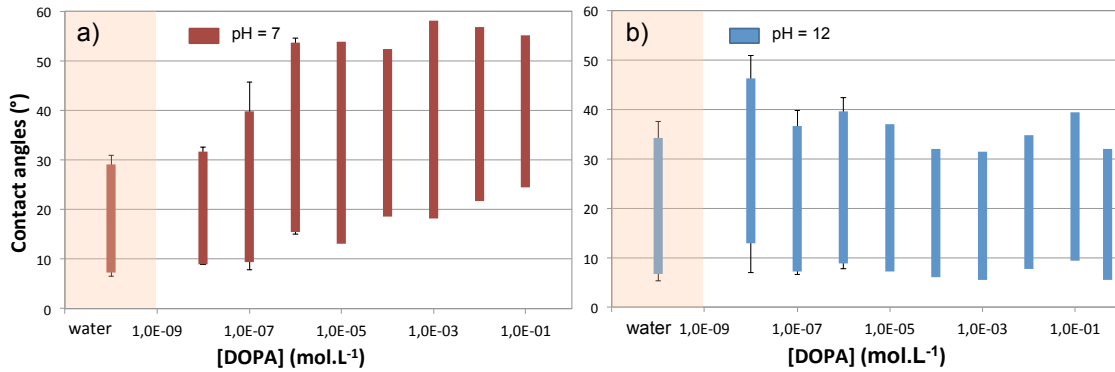


Figure 11: Advancing and receding angles on glass depending on the dopamine concentration, at $\text{pH}=7$ (a) and 12 (b). At $\text{pH}=7$, contact angle increases with dopa concentration up to 10^{-6}mol.L^{-1} , above which angles seem independent of $[\text{DOPA}]$, suggesting that the dopamine coating is less hydrophilic than the raw glass. This effect disappears at $\text{pH}=12$, the dynamic contact angles do not vary significantly over the whole range of concentrations of dopamine explored.

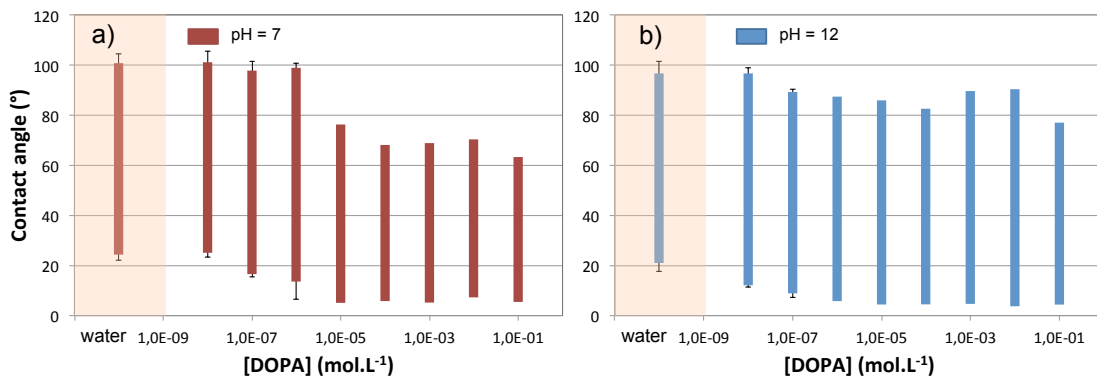


Figure 12: Advancing and receding angles on stainless steel (without polishing) depending on the dopamine concentration, at $\text{pH}=7$ (a) and 12 (b). For $\text{pH}=7$, dopamine coating leads to a decrease of both the advancing and receding angles, suggesting that the dopamine coating is more hydrophilic than the raw steel. The variation seems to stabilize above the predicted $C_{crit} \simeq 10^{-5}\text{mol.L}^{-1}$. At $\text{pH}=12$, the effect of the dopamine is more subtle but indeed present since we go from an hydrophobic situation for the pure water (advancing angle $>90^\circ$) to a slightly hydrophilic one for dopamine solution with a concentration above 10^{-7}mol.L^{-1} .

The same experiments were run on stainless steel. At pH=7 [Fig.12(a)] we also see a notable change in the values of the angles, this time above 10^{-5}mol.L^{-1} , with angles going from 100° (advancing) and 23° (receding) for pure water, to 63° and 6° for highly concentrated dopamine solutions. At pH=12 [Fig.12(b)] the variation is less important, going from 95° and 21° for the reference to 79° and 6° for the most concentrated solutions. Though this second variation is smaller, we still move from a slightly hydrophobic situation (advancing angle above 90°) to a slightly hydrophilic one. This hydrophobic situation is actually problematic: steel should not display such properties (metals have a high surface energy, way higher than the surface tension of the water, so a water droplet should spread) [14]. There must have been some pre existing coating on the steel that resisted the sonication and the organic solvents. Therefore we tried again with the same sample but polished to a roughness of about $1\ \mu\text{m}$, allowing us to control the roughness and to be sure that the surface is not already coated. Since the variations of the contact angles are more important at pH=7, we will fix the parameter from now on. Results are showed in Fig. 13(a).

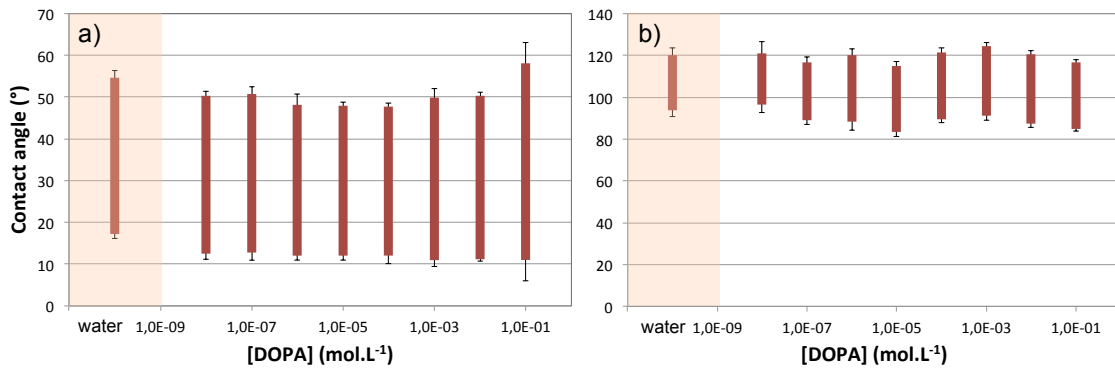


Figure 13: (a) Advancing and receding angles on polished steel versus dopamine concentration. No change in the contact angles is observed over the range of concentrations explored. (b) Advancing and receding angles on polished Teflon display higher angles than on polished steel or glass because of the hydrophobicity of the material, but do not change either with the dopamine concentration.

For the experiments done with the dopamine solutions on the polished steel, there does not seem to be any change at pH=7 and the angles values are consistently 50° and 12° . This was a surprise: we expected a drastic change from the hydrophobic behavior of the unpolished "steel" but dopamine as been shown to stick on metallic substrates [12]. Therefore we suspected that the timescale of our measure did not allow for the dopamine to react on our substrates. As a control to make sure that the effects observed are due to the dopamine interaction with the substrate, the last of these tests was performed on polished Teflon (same roughness), a surface known for being very difficult to adhere on. This time the values of the angles are obviously much higher than for the other tests on glass or polished steel (Teflon is a more hydrophobic substrate), but stays constant when the concentration of dopamine increases.

3.2 Multiple hysteresis cycles

Because during the first set of tests, differences have been observed when droplets were tested twice on the same spot, we decided to try multiple cycles of adding and withdrawing liquid at a same location. In Fig. 14 is an explanation of how these experiments were conducted and of how to read the resulting graph (Fig. 15). On this example of an experiment run of polished steel, each successive droplet was slightly bigger than the previous one, hence the progression toward the right on the graph. The 13 different cycles of droplets of a 10^{-1}mol.L^{-1} dopamine solution are displayed. The blue, green and orange color codes correspond to sets of droplets that had the same volume, *i.e.* explored the same region on the substrate. For each of those groups, we can see a progressive decrease of the advancing angle with the number of cycles. On the 4th cycle for instance (deep blue), the steps marking each previous stops are clearly visible and show that the advancing contact angle value decreases when the time of exposition of the substrate to dopamine increases.

We furthermore ran two control tests to make sure that we are indeed monitoring the effect of the creation of a dopamine layer onto the substrate. First the same dopamine solution (10^{-1}mol.L^{-1}) on polished Teflon [Fig. 16(a)] ; and second pure water on the same polished steel [Fig. 16(b)]. In both cases, the number of cycles does not seem to play a role. The first control assures us that there is a need for

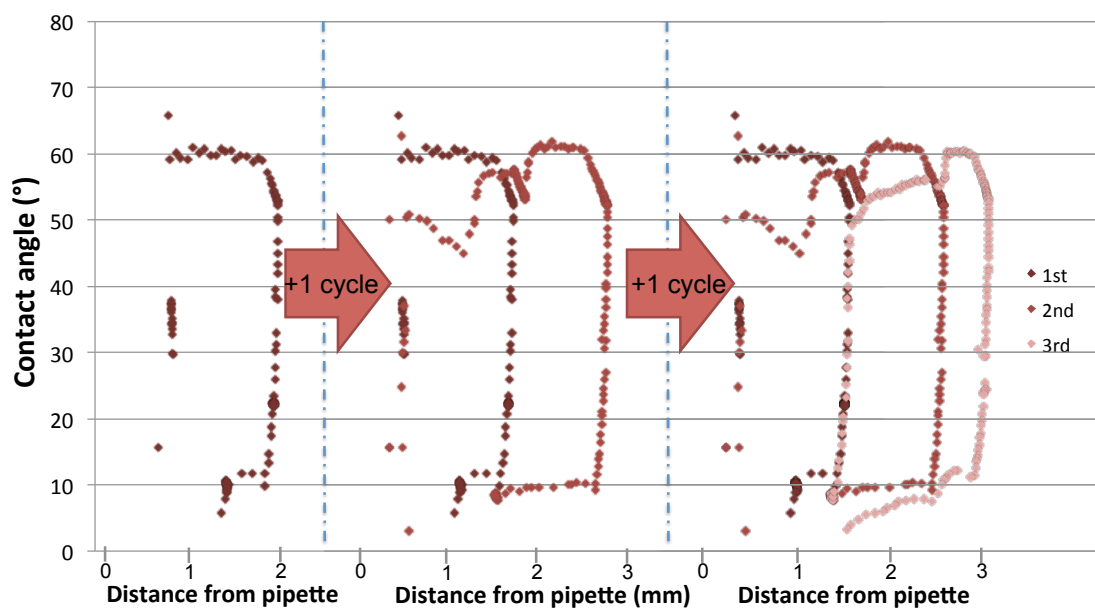


Figure 14: Multiple hysteresis cycles on steel $[DOPA]=10^{-1}\text{mol.L}^{-1}$, $\text{pH}=7$. For each cycle, the advancing and receding angles are shown, versus their distance from the pipette. The bigger the droplet, the further the angle measured are from the pipette.

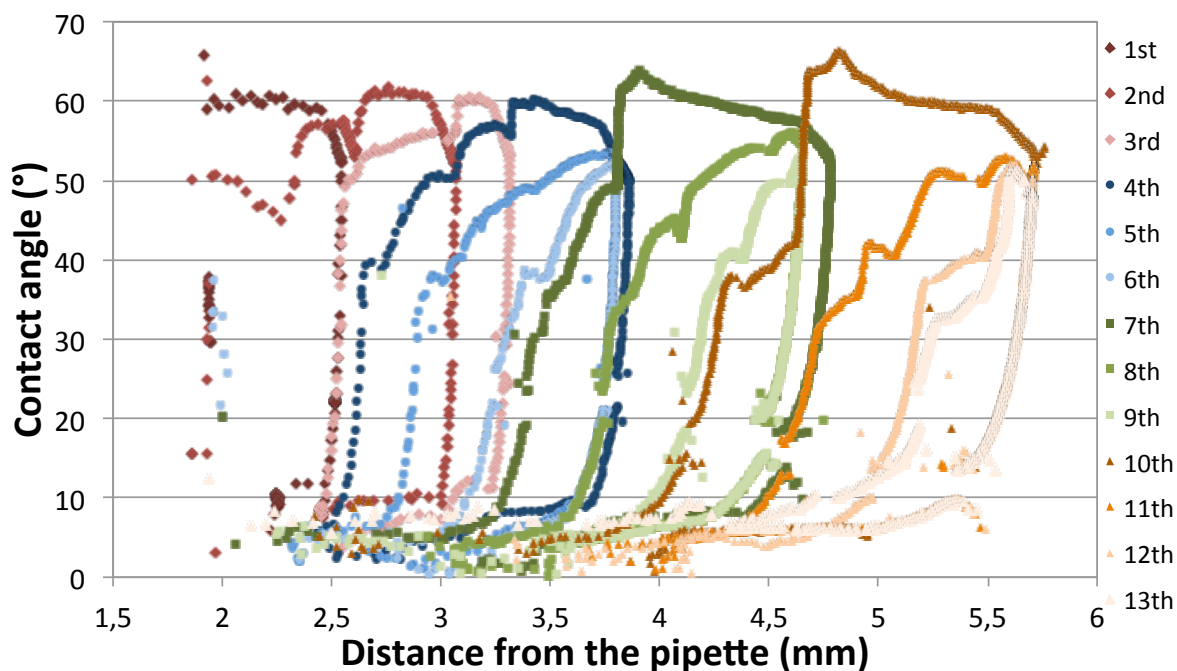


Figure 15: 13 successive hysteresis cycles on polished steel $[DOPA]=10^{-1}\text{mol.L}^{-1}$, $\text{pH}=7$. For a given distance from the pipette, it is clear that the advancing angle decreases each cycle. Close to vertical lines mark the pinning of the droplet.

a dopamine-substrate interaction to see a change in the contact angles over time, and that this change is not caused by some reaction of the dopamine with itself in the solution. The second control tells us that the variation of the advancing angle over time is not due to a layer of water being adsorbed in the remaining asperities of the substrate.

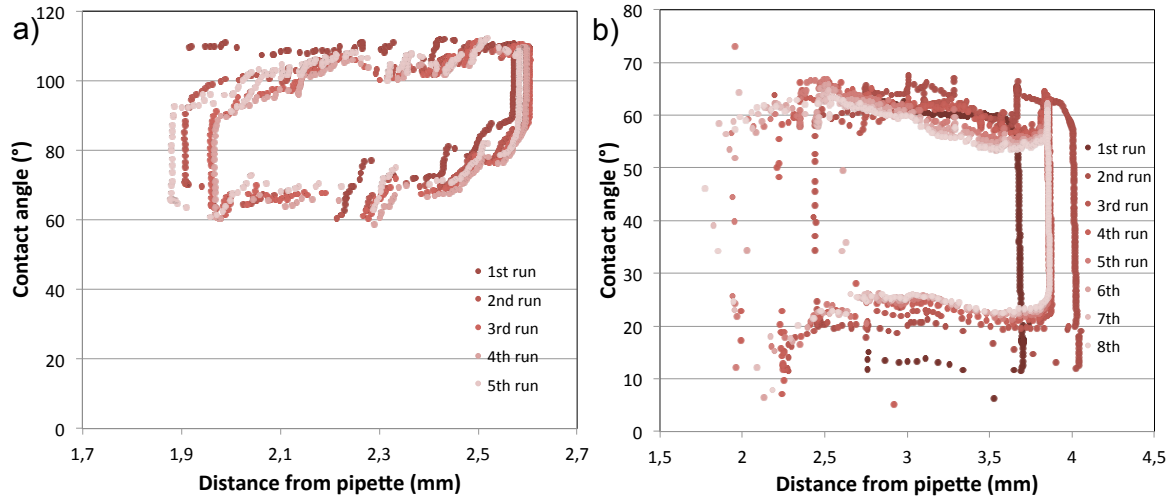


Figure 16: (a) First control : multiple cycles with a dopamine solution ($[DOPA]=10^{-1}\text{mol.L}^{-1}$, $\text{pH}=7$), on Teflon. There is no significant change between the cycles, except a step-like behaviour for the receding angle but this is likely caused by some dust that pinned the droplet. (b) Second control : multiple cycles with deionized water on polished steel (surface roughness $\simeq 1\mu\text{m}$). The absence of change between the cycles shows that the effect observed with the dopamine does not come from a layer of water trapped in asperities of the substrate.

3.3 Time dependence of the angle

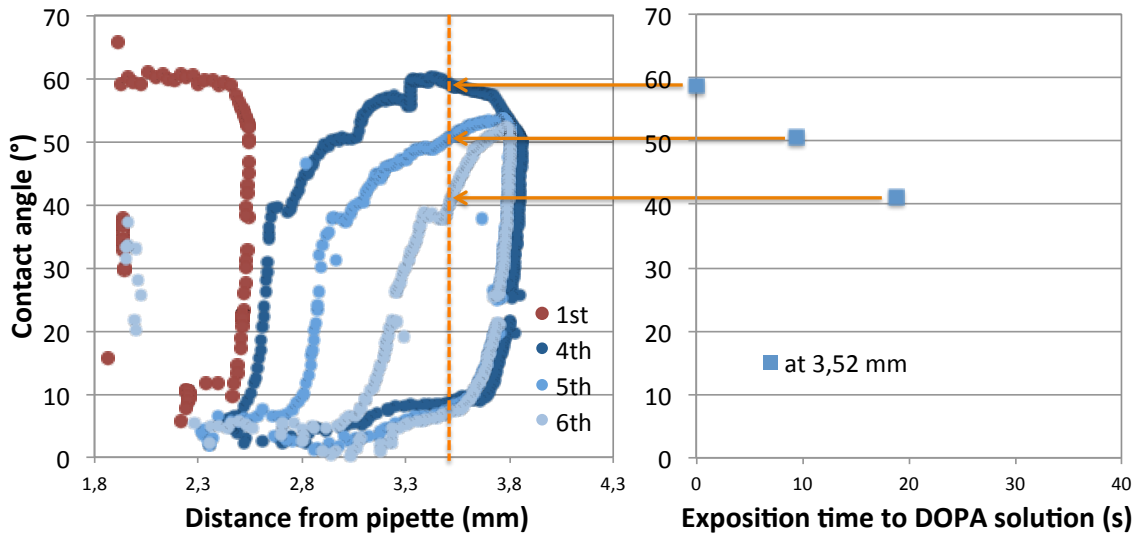


Figure 17: Creation of the time-resolved graph by fixing a position and looking at the time this position has been exposed to the dopamine solution previously, for each cycle (every point being separated by 200 ms). Multiple vertical cuts allow for a larger spectrum of angles.

In order to better capture the time dependence of the decrease observed for advancing angles in Fig. 15, we generated a time-resolved graph by fixing a distance from the pipette and plotting, for each cycle, the angle at this position versus the duration of exposition to the dopamine during previous cycles (Fig. 17). By taking several vertical cuts, we were able to plot Fig. 18(a). We see that the advancing angles decrease as what could be an exponential over a few hundreds of seconds.

$$\theta(t) = \theta_0 - (\theta_0 - \theta_\infty)(1 - e^{-t/\tau}) \quad (9)$$

The best fit was found using Matlab fitting tool and by letting θ_∞ and the exponential rate τ free. We did the same process for a less concentrated (10^{-2}mol.L^{-1}) dopamine solution : the different cycles as

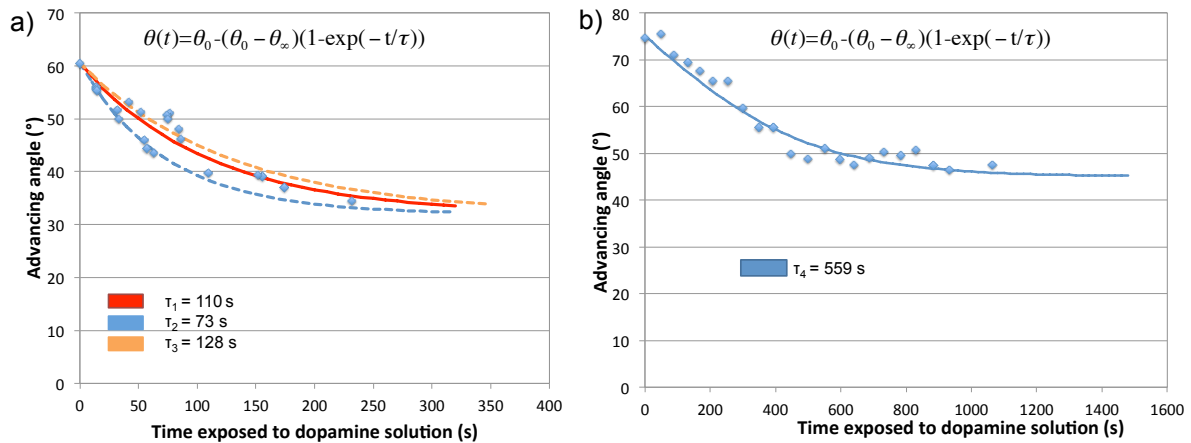


Figure 18: Advancing angles displayed as a function of the time of exposition to the dopamine solution prior to the measurement. (a) Measure for a $10^{-1} \text{ mol.L}^{-1}$ dopamine solution on polished steel. Points come from cycles 4 to 13 of the experiment Fig. 15. The red curve is the best fit using the exponential decay displayed and every point for the experiment. Orange (resp. blue) dashed curve is the best fit using only points from orange (resp. blue) cycles of Fig. 15, *i.e.* the further (resp. closer) from the pipette. (b) Similar experiment for a $10^{-2} \text{ mol.L}^{-1}$ dopamine solution on polished steel. All the fitting parameters τ_i are recorded with their color code.

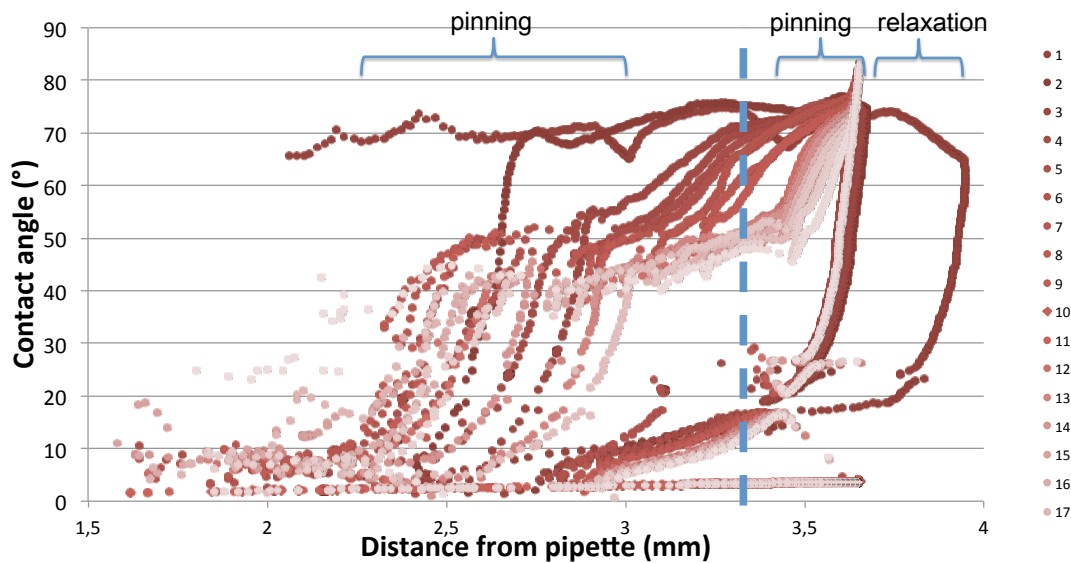


Figure 19: Multiple cycle for a dopamine solution ($10^{-2} \text{ mol.L}^{-1}$). Each successive droplet has the same size except the first, which is slightly larger. Unacceptable zone for measures are displayed, and the vertical cut used for Fig. 18 is marked by the vertical dashed line.

well as the "vertical cut" chose are shown in Fig. 19 and the temporal evolution of the advancing angle is displayed in Fig. 18(b). The place where the vertical cuts are made is a difficult choice. We must not take points in the sharp increase before the receding part of a cycle because it corresponds to a pinning of the droplet. For the same reason, points during the jump at the beginning of the advancing part are also to be avoided. The reason pinning events are not vertical lines as they should is that we take the angle value from one side and the x-axis values on the graphs are actually half the size of the droplet, and the droplet can continue to grow on the other side while pinning happens on the side where we measure the angle. Finally, one can see (for instance in Fig. 19, on the 1st cycle) that before the drop preceding the receding angles, the value of the angle starts to decrease while the drop is still expanding. This change in the angle actually happens while the volume is constant. But because the angle needs to reach its (lower) equilibrium value (not necessarily Young's value !), the drop must keep expanding. Those points also can not be taken into account.

In Fig. 18 (a) and (b), we plotted every point corresponding to the vertical cuts showed in Fig. 17

and Fig. 19 for both concentrations, and tried one fit with an exponential function. The factors deduced from the regression are displayed with the same color code than the curves. The characteristic decay time for the advancing angles of the 10^{-2}mol.L^{-1} solution is much longer than the one for the 10^{-1}mol.L^{-1} solution. On the test with the 10^{-1}mol.L^{-1} , we furthermore observed that the angles measured closer from the pipette (blue) decrease faster than the one the furthest (orange).

4 Discussion

4.1 Kinetics of adsorption

The results presented here confirm that the study of the contact angles is a relevant way of obtaining information about the dopamine deposition on a substrate and especially about the adsorption dynamics and the formation of a coating. There were no doubts from the start that dopamine would bind to the substrates investigated [12], but the series of experiments with different concentrations assured us that the changes on the surface had enough impact on the contact angles for us to be able to monitor it, both in highly wetting conditions (glass, Fig. 11) and poorly wetting conditions (hydrophobic "steel", Fig. 12). In both cases, the advancing angles converged at high dopamine concentrations towards 60° . Because the contact angle depends on the three surface energies γ_i , we made sure that the effect did not come from a change in the liquid-vapor surface tension γ_{LV} by testing the evolution of the angle on Teflon [Fig. 13 (b)]. The lack of significant change in the angles values with the concentration allowed us to conclude that γ_{LV} was not affected significantly by the change in dopamine concentration (no surfactant effect).

This value of 60° is then likely to be the value of a dopamine solution on a layer of dopamine. The convergence of the values observed between the two substrates above 10^{-5}mol.L^{-1} [which was the packed molecule saturation threshold calculated in the introduction, Eq. (8)] led us first to think of this value as the unique value of advancing angle of water on a dopamine film. But we observed that multiple cycles on the same spot of a sample led to different results : the advancing angle was lowered. A more careful investigation of this temporal variation (Fig. 18) showed that the advancing angle was indeed decreasing with the exposition time, from the angle reported in Fig. 13 (a) to an angle θ_∞ , which seems dependent of the concentration (32° for 10^{-2}mol.L^{-1} and 40° for 10^{-1}mol.L^{-1}). This means that a longer exposition to the dopamine solution leads to a different surface state, and that that state depends on the concentration of the solution. This is consistent with the results from Ball *et al.* [15], who found that the size of the polydopamine film deposited on silicon from a dopamine solution was linearly correlated to the concentration of the dopamine solution : the final film resulting from the exposition to the 10^{-2}mol.L^{-1} dopamine solution is thinner than the one with the 10^{-1}mol.L^{-1} solution. The other result from that experiment is the rate at which the advancing angle decreases. Characteristic times are deduced from a fit using an exponential function. Though we do not have a real model justifying the use of this function, this choice was suggested by the kinetics of formation of a dopamine layer on silicon [15]. We see that the rate seems to be smaller when we get further away from the syringe [Fig. 18]. This could be due to the fact that by coating the central zone, we actually consume part of the dopamine and the actual concentration decreases. For the 10^{-1}mol.L^{-1} solution, the characteristic time observed for the furthest points (orange dashed line) is actually almost twice as long as the timescale involved for the closest points (blue dashed line). Assuming a linear relation between decreasing rate and concentration, that could give us an idea of the size of the layer : characteristic time is multiplied by 5 when the concentration is divided by 10, so if the timescale is multiplied by 2, the concentration has been divided by 4. If the droplet is 1 cm^2 large and 1 mm thick, a monolayer of packed molecules of 30 nm uses 10^{15} molecules while there are 6.10^{18} molecules in the droplet. Using $3/4$ of the molecules ($4.5.10^{18}$) of the droplet (assuming the concentration homogeneous), requires roughly 4500 layers or 70 nm in a bulk ($10^{-9}\text{m} \cdot 4500^{1/2} = 7.10^{-8}\text{m}$), which is consistent with the thickness observed by Ball *et al.*, but this thickness is reached much faster ($\sim 10^3\text{ s}$ for us on steel versus $\sim 10^4\text{ s}$ on silicon, with 10^{-2}mol.L^{-1} dopamine solution in both cases). Now this average thickness is actually not a homogeneous thickness : after the experiment and letting dry the surface, we start seeing the coating (Fig. 20), with a coffee stain effect on the edge, and direction where the coating seemed facilitated.

We tried running this experiment for an even lower concentration (10^{-3}mol.L^{-1}) but the timescale involved was such that we started to have some evaporation, which made the control of the volume complicated. One problem though is the fact that the layer induces some uncontrolled roughness and this roughness will have an contrary effect on the angle. Wenzel [16] showed that geometrical roughness increased the contact angle following the relation

$$\cos(\theta) = r \cdot \cos(\theta_Y) \quad (10)$$

where

$$r = \frac{\text{actual surface}}{\text{apparent surface}} \quad (11)$$

But the post polishing roughness being at best $1 \mu\text{m}$, we can hope that this effect is negligible. The obvious control experiment that should be performed to verify those results would be to dip-coat our steel in a dopamine solution for different times and verify the rates with pure water. That would hopefully create a more regular coating and make sure that the concentration of the droplet does not change with the radius.

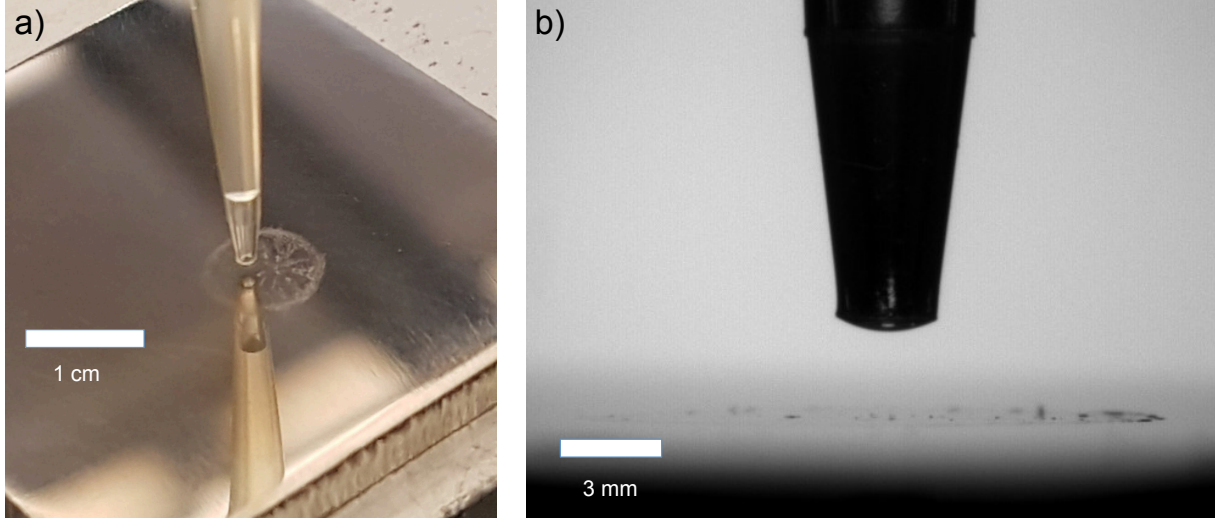


Figure 20: Pictures of the polydopamine coating after the multiple cycles test with the 10^{-1}mol.L^{-1} dopamine solution and after evaporation. (a) top view, (b) side view using the goniometer.

4.2 Back to adhesion energy

The initial idea behind this project was to evaluate the adhesion energy of the dopamine on a solid substrate. Equilibrium contact angles and surface energy are connected through Young's equation. Besides, Tadmor [17] showed how advancing and receding angles together allow to predict Young's angle value assuming that the irregularities on the surface are isotropic in nature and distribution (so that the resistance to the motion is the same for advancing and receding angle) :

$$\theta_Y = \arccos \left(\frac{\Gamma_R \cdot \cos(\theta_R) + \Gamma_A \cdot \cos(\theta_A)}{\Gamma_R + \Gamma_A} \right) \quad (12)$$

where Γ_R and Γ_A are defined as :

$$\Gamma_R = \left(\frac{\sin(\theta_R)^3}{(2 - 3 \cos(\theta_R) + 3 \cos(\theta_R)^3)} \right)^{1/3} ; \quad \Gamma_A = \left(\frac{\sin(\theta_A)^3}{(2 - 3 \cos(\theta_A) + 3 \cos(\theta_A)^3)} \right)^{1/3} \quad (13)$$

So in theory, given the advancing and receding angle, we can infer Young's angle and if we know the two other surface tensions, we have the γ_{LS} and with the size of the molecule, that may gives us an idea of the adhesion energy. But if we look at the order of magnitude of the different γ , we see that $\gamma_{SV} \simeq 2 \text{ J.m}^{-2}$ whereas $\gamma_{LV} \simeq 70 \text{ mJ.m}^{-2}$. So :

$$\gamma_{LS} \in [\gamma_{SV} - \gamma_{LV} ; \gamma_{SV} + \gamma_{LV}] \longrightarrow \gamma_{LS} = \gamma_{SV} \pm 1\% , \quad (14)$$

which means that the important measure is the measure of γ_{SV} . This measure using contact angles (and the Owens-Wendt model) relies on assumptions as to what types of interaction the substrate is capable of making [18]. Reference liquid such as water, ethylene glycol, diiodomethane, formamide, glycerol are to be used because the interaction they are susceptible to make are well known. Such measures have not been conducted during this internship and would need careful work but if we bluntly use values quoted earlier from the literature[ref], we find an energy per dopamine (still assuming packed molecules) of about 102 kJ.mol^{-1} , which is indeed the correct order of magnitude compared to the AFM value [6].

5 Conclusion

This contact angle method provided us with some promising results concerning the adsorption kinetics of dopamine on steel, and could most likely also work with glass since we have also showed how much dopamine coating changed the contact angle of aqueous solutions on glass. But we mostly showed how this very simple method provides relevant information on these dynamics. Provided a calibration using another quantitative method to measure film deposition (ellipsometry for instance [15] ; [19]), advancing contact angle measurement could be an effective and easy way to monitor such phenomena. As for the adhesion energy, the problem seems more complex, and surface energy of our samples would need to be measured before drawing any other conclusion.

References

- [1] J Herbert Waite. Mussel adhesion—essential footwork. *Journal of Experimental Biology*, 220(4):517–530, 2017.
- [2] Steven W Taylor, Bernd Kammerer, and Ernst Bayer. New perspectives in the chemistry and biochemistry of the tunichromes and related compounds. *Chemical reviews*, 97(1):333–346, 1997.
- [3] Jing Yu, Wei Wei, Eric Danner, Jacob N Israelachvili, and J Herbert Waite. Effects of interfacial redox in mussel adhesive protein films on mica. *Advanced materials*, 23(20):2362–2366, 2011.
- [4] Qiang Wei, Fulong Zhang, Jie Li, Beijia Li, and Changsheng Zhao. Oxidant-induced dopamine polymerization for multifunctional coatings. *Polymer Chemistry*, 1(9):1430–1433, 2010.
- [5] Jing Yu, Yajing Kan, Michael Rapp, Eric Danner, Wei Wei, Saurabh Das, Dusty R Miller, Yunfei Chen, J Herbert Waite, and Jacob N Israelachvili. Adaptive hydrophobic and hydrophilic interactions of mussel foot proteins with organic thin films. *Proceedings of the National Academy of Sciences*, page 201315015, 2013.
- [6] Haeshin Lee, Norbert F Scherer, and Phillip B Messersmith. Single-molecule mechanics of mussel adhesion. *Proceedings of the National Academy of Sciences*, 103(35):12999–13003, 2006.
- [7] Niels Holten-Andersen, Thomas E Mates, Muhammet S Toprak, Galen D Stucky, Frank W Zok, and J Herbert Waite. Metals and the integrity of a biological coating: the cuticle of mussel byssus. *Langmuir*, 25(6):3323–3326, 2008.
- [8] Stephan Schönecker, Xiaoqing Li, Börje Johansson, Se Kyun Kwon, and Levente Vitos. Thermal surface free energy and stress of iron. *Scientific reports*, 5:14860, 2015.
- [9] TA Roth. The surface and grain boundary energies of iron, cobalt and nickel. *Materials Science and Engineering*, 18(2):183–192, 1975.
- [10] Jae Yoon Park, Jihyeon Yeom, Jee Seon Kim, Mihyun Lee, Haeshin Lee, and Yoon Sung Nam. Cell-repellant dextran coatings of porous titania using mussel adhesion chemistry. *Macromolecular bioscience*, 13(11):1511–1519, 2013.
- [11] John P Evans, Kyunghye Ahn, and Judith P Klinman. Evidence that dioxygen and substrate activation are tightly coupled in dopamine β -monooxygenase implications for the reactive oxygen species. *Journal of Biological Chemistry*, 278(50):49691–49698, 2003.
- [12] Haeshin Lee, Shara M Dellatore, William M Miller, and Phillip B Messersmith. Mussel-inspired surface chemistry for multifunctional coatings. *science*, 318(5849):426–430, 2007.
- [13] Tommi Huhtamäki, Xuelin Tian, Juuso T Korhonen, and Robin HA Ras. Surface-wetting characterization using contact-angle measurements. *Nature protocols*, page 1, 2018.
- [14] Malcolm E Schrader. Wettability of clean metal surfaces. *Journal of colloid and interface science*, 100(2):372–380, 1984.
- [15] Vincent Ball, Doriane Del Frari, Valérie Toniazzo, and David Ruch. Kinetics of polydopamine film deposition as a function of ph and dopamine concentration: insights in the polydopamine deposition mechanism. *Journal of colloid and interface science*, 386(1):366–372, 2012.
- [16] Robert N Wenzel. Resistance of solid surfaces to wetting by water. *Industrial & Engineering Chemistry*, 28(8):988–994, 1936.
- [17] Rafael Tadmor. Line energy and the relation between advancing, receding, and young contact angles. *Langmuir*, 20(18):7659–7664, 2004.
- [18] Anna Rudawska and Elżbieta Jacniacka. Analysis for determining surface free energy uncertainty by the owen–wendt method. *International Journal of Adhesion and Adhesives*, 29(4):451–457, 2009.
- [19] JO Zerbino and MG Sustersic. Ellipsometric and electrochemical study of dopamine adsorbed on gold electrodes. *Langmuir*, 16(19):7477–7481, 2000.